

# Coastal phytoplankton bloom dynamics in the Tyrrhenian Sea: Advantage of integrating in situ observations, large-scale analysis and forecast systems

R. Martellucci<sup>a,b,c,\*</sup>, S. Salon<sup>a</sup>, G. Cossarini<sup>a</sup>, V. Piermattei<sup>b,c</sup>, M. Marcelli<sup>b,c</sup>

<sup>a</sup> National Institute of Oceanography and Applied Geophysics – OGS, Italy

<sup>b</sup> CMCC-OPA, Italy

<sup>c</sup> Laboratory of Experimental Oceanology and Marine Ecology, DEB - University of Tuscia, Italy

## ARTICLE INFO

### Keywords:

Phytoplankton  
Annual cycle  
Spring blooms  
Physical forcing  
Multiplatform approach

## ABSTRACT

Coastal systems represent the most dynamic natural systems on Earth, making their study particularly challenging. A holistic approach that integrates a set of monitoring tools for data collection (i.e., satellite imagery, numerical models and in situ observations) may provide different information about coastal ecosystems at different spatial and temporal scales. Of course, none of these tools are perfect, being that each is characterized by intrinsic errors and therefore specific uncertainties, which is also an important subject of investigation.

Long-term high-resolution in situ observations of the phytoplankton biomass at a coastal site (Civitavecchia, Tyrrhenian Sea), provided by the Civitavecchia Coastal Environment Monitoring System (C-CEMS) observational platform, are presented, discussed and integrated with data from the Copernicus Marine Environment Monitoring Services (CMEMS) for the Mediterranean Sea, which are generated by the MedBFM model system, and satellite observations from the CMEMS Ocean Colour database. The analysis of the time series of phytoplankton provided by in situ, satellite and model data show the typical dynamics of coastal temperate systems, which are characterized by spring and autumn blooms and significant interannual variability. The empirical orthogonal function (EOF) analysis highlights the consistency among the multiplatform datasets, whereas integrating the local in situ time series with a spatial analysis from model and satellite data provides information about the extent of coastal bloom phenomena and the relevance of the observation location with respect to surroundings. Our study of the dynamics of coastal blooms in the Civitavecchia coastal system allows us to propose a best practice framework that may be of general interest, and potentially applied to any multiplatform monitoring system (MPMS). The MPMS approach allows us to investigate the interannual variability over different horizontal and vertical scales, reflecting the variability in natural drivers (i.e., atmospheric forcings, coastal currents, upwelling, and land inputs), as typically expected in coastal areas.

## 1. Introduction

Coastal systems are among the most dynamic natural systems, where chemical, physical and biological processes interact at different spatial and temporal scales (Walsh, 1988, 1991; Gattuso et al., 1998; Liu et al., 2000; Ducklow and McCallister, 2005; Muller-Karger et al., 2005). Approximately 40% of the world's population lives in land-sea transition zones (Seibert et al., 2020), increasing human pressure, modifying the normal characteristics of coastal systems and causing a series of detrimental effects (e.g., eutrophication and harmful algal blooms). Quantification of the state of the marine environment (sensu MSFD; Oesterwind et al., 2016) is necessary to understand anthropogenic

impacts and separate them from natural fluctuations (Hardman-Mountford et al., 2005; Allen et al., 2007).

The new and emerging ecosystem-based management method proposed by the Marine Strategy Framework Directive (2008/56/EC) suggests implementing the monitoring of coastal systems by using different observation platforms, which would provide information on the space-time distribution of major parameters related to water quality (Oinonen et al., 2016).

Following such an approach, we aim to understand the spatial and temporal distributions of phytoplankton biomasses in coastal waters to evaluate the evolution of phytoplankton dynamics in a coastal polluted area located in the northern Tyrrhenian Sea. Indeed, as also suggested by

\* Corresponding author at: National Institute of Oceanography and Applied Geophysics – OGS, Italy.

E-mail address: [rmartellucci@inogs.it](mailto:rmartellucci@inogs.it) (R. Martellucci).

<https://doi.org/10.1016/j.jmarsys.2021.103528>

Received 10 June 2020; Received in revised form 12 December 2020; Accepted 16 February 2021

Available online 25 February 2021

0924-7963/© 2021 Elsevier B.V. All rights reserved.

the MSFD (e.g., descriptors 1, 4 and 5), chlorophyll *a* concentrations and the consequent phytoplankton blooms enable us to understand the ecosystem status (Hays et al., 2005; Cloern and Jassby, 2010).

It is well known that phytoplankton growth and the related increase in biomass (i.e., blooms) are controlled by light energy availability and nutrient supply (Cloern, 1996; Lévy et al., 1998). Moreover, phytoplankton growth is strictly related to the physical forcing (Legendre and Demers, 1984; Kjørboe and Nielsen, 1990) that drives coastal current and runoff dynamics, which will influence primary producer succession in marine environments (Margalef, 1978; Lennert-Cody and Franks, 2002). In coastal waters, environmental forcings (e.g., wind, rain, rivers, waves, and tides) present the highest variability, and phytoplankton growth strictly depends on this variability (Franks and Walstad, 1997), making an understanding of phytoplankton dynamics extremely difficult to obtain.

The focus of this work is twofold: first, we are interested in analysing the phytoplankton bloom dynamics of the Civitavecchia coastal ecosystem by adopting a multiplatform approach that integrates the Copernicus Marine Environment Monitoring Services (CMEMS) products and the C-CEMS (Civitavecchia Coastal Environment Monitoring System; Bonamano et al., 2016) in situ data. Second, we aim to propose best practices to integrate multiplatform data streams that may also be adopted in other similar contexts of coastal ecosystems.

CMEMS is part of the EU Copernicus programme services ([www.cope](http://www.cope)

[marine.copernicus.eu](http://marine.copernicus.eu)) and is devoted to the monitoring and forecasting of the marine environment, operationally providing free-access, standardized, quality-validated data and information on ocean state (physics, biogeochemistry and sea ice). CMEMS products are available to users through a digital catalogue (<http://marine.copernicus.eu/services-portfolio/access-to-products/>), which includes near real time and reprocessed observations from satellite and reanalysis, analysis and short-term forecasts from global and regional models. An exhaustive description of the CMEMS architecture and further details on the service can be found in Le Traon et al. (2019).

Integrating multi-sensor and multiplatform data streams requires a preliminary analysis of their consistency with respect to the spatial and temporal scales of the investigated dynamics. As a reference, in Mozetič et al. (2010), satellite and in situ chlorophyll are compared for consistency at several representative stations before investigating the chlorophyll multidecadal trend in the Northern Adriatic Sea.

The paper is organized as follows: Section 2 describes the study area and the multiplatform datasets, and Section 3 shows the results concerning phytoplankton dynamics. A discussion is provided in Section 4, and concluding remarks are provided in Section 5.

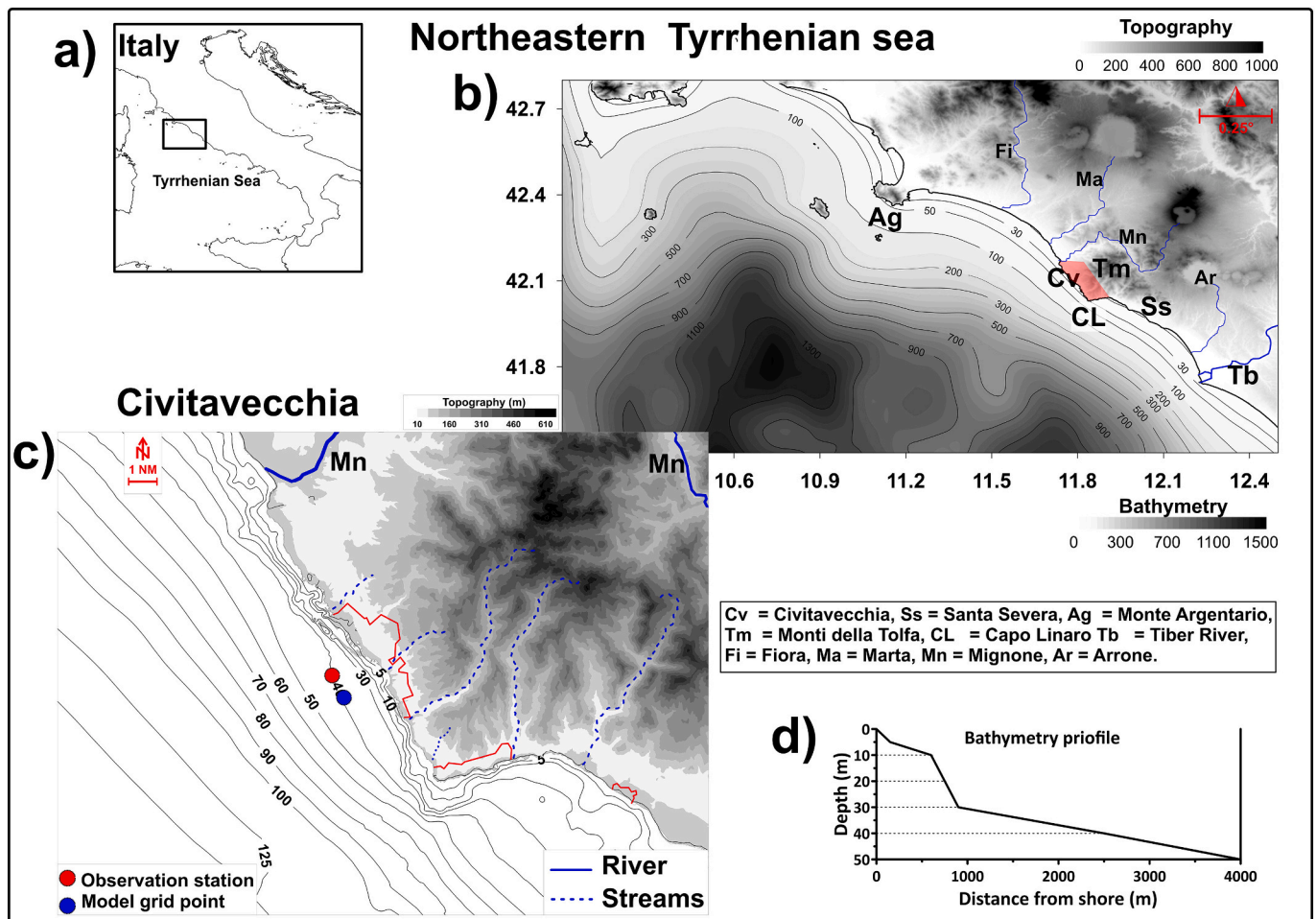


**Fig. 1.** Location of the study area (a); bathymetry and orography of the north eastern Tyrrhenian coast (b) with geographical details of the study area: cities, Civitavecchia (Cv) and Santa Severa (Ss); mountains, Monte Argentario (Ag), Capo Linaro (CL) and Monti della Tolfa (Tm); rivers, Tiber (Tb), Fiora (Fi), Marta (Ma) and Mignone (Mn). Map (c) of the Civitavecchia coastal area (red area in b), inclusive of streams (blue dashed line) and rivers (blue lines), urban areas (delimited by red lines) and the location of the observation station and model grid point and the bathymetry profile (d, see inset). (For interpretation of the references to colour in this figure legend, the reader is referred to the web version of this article.)

## 2. Material and methods

### 2.1. Study area

The coastal area of Civitavecchia (Fig. 1c) is in the northeastern part of the Tyrrhenian Sea (Fig. 1a and b). The Tyrrhenian Sea is affected by mesoscale circulation and significant seasonal variability (Hopkins, 1988; Pinardi and Navarra, 1993; Marcelli et al., 2005; Vetrano et al., 2010; Poulain et al., 2012; Iacono et al., 2013; de la Vara et al., 2019) and can be considered the most isolated basin in the western Mediterranean (Astraldi and Gasparini, 1994) due to its morphodynamic characteristics. The coastal area of Civitavecchia is a populated area characterized by the coexistence of industrial and human pressures with environmental resources and values. This area hosts a harbour that is one of the largest in Europe in terms of traffic of vessels (Zappalà et al., 2014; Paladini de Mendoza et al., 2016) and industrial activities, including power plants and farms. In particular, extended agricultural activities may significantly influence nutrient dynamics along the coast. In addition, over the last 20 years, urban expansion has led to an increase in urban wastewater discharge into seawater through four major outputs (Tb, Fi, Ma and Mn in Fig. 1b) and streams (Fig. 1c) located along the coastline (Bonamano et al., 2015; Zappalà et al., 2016; Piazzolla et al., 2020).

The study area (Fig. 1b) is delimited in the northern part by the physiographic unit that extends from Capo Lınaro to Monte Argentario and in the southern part by the physiographic unit extended from Capo Lınaro to Capo Anzio (Anselmi et al., 1978; Scanu et al., 2015). The topography behind the coastline is characterized by the presence of mountains interspersed with floodplains (Brondi et al., 1979); this complex configuration provides a natural barrier against air masses modifying the evolution of synoptic winds (Astraldi et al., 1995).

From a morphological point of view, the coastal area may be divided into two sectors separated by Capo Lınaro (Fig. 1b): the northern portion is steep with rocky outcrops (Chiocci and La Monica, 1996; La Monica and Raffi, 1996), and the southern portion is characterized by a smoother seabed with sandy and gravel beaches. The mainland behind Civitavecchia includes the Tolfa Mountains, which reach a maximum height of approximately 600 m.

Along the study area, some rivers and streams regulate runoff dynamics (Fig. 1b and c). The Tiber River, the most important river on the western coast of Italy, presents the highest solid load discharge in the southern part of the area. The northern part of the study area receives alluvial deposits from river basins (Fig. 1b) and from several small streams (Fig. 1c), which affect marine sedimentation locally and during strong flood events (Scanu et al., 2015; Piazzolla et al., 2015).

The mean alongshore flow at Civitavecchia is directed northwestwards along the coast and is characterized by a significant amount of variability at a timescale of 2–3 days (Elliot, 1981; Martellucci et al., 2018). The study area presents a spring tidal range of  $\pm 0.3$  m (Paladini de Mendoza et al., 2018), whereas as observed by Paladini de Mendoza et al. (2016), the wave heights are at the maximum in autumn and winter seasons ( $H_m^0 > 3$  m), originating more frequently in the south-western sector. The wind in the study area shows two prevailing directions over the year from South/East ( $110^\circ\text{N}$ – $140^\circ\text{N}$ ) and North/Northeast ( $0^\circ\text{N}$ – $60^\circ\text{N}$ ). The winds blowing from the South/East favour downwelling, and those from the North/Northeast produce upwelling (Bakun and Agostini, 2001; Martellucci et al., 2020): these coastal wind-driven currents modulate the variability in the investigated study area.

Studies of coastal phytoplankton dynamics in the Tyrrhenian coastal zone are very limited, especially those related to our study area, which were most recently performed between the 1980s and 1990s (Lenzi and Lazzara, 1980; Innamorati et al., 1990; Innamorati et al., 1992; Nuccio et al., 1995). Observations from those studies showed that the annual cycle of phytoplankton was typical for temperate regions, with two annual blooms that occurred during the early spring (February–April) and autumn (September–November) and similar to what was found by

De Angelis (1956), the absence of a regular summer bloom. However, some blooms between June and July were observed by Solazzi and Andreolli (1971), Magazzù et al. (1975) and Bernhard et al. (1969). During the year, diatoms and dinoflagellates alternate, following the classic paradigm (Margalef et al., 1969) characterized by diatoms during the cold seasons (autumn winter and early spring) and dinoflagellates in the warmer season; in every case, diatoms prevail both in biomass and species.

### 2.2. Multiplatform data streams: in situ, model and satellite datasets

We analysed the phytoplankton dynamics in coastal waters through the in situ measurement dataset gathered by the Civitavecchia Coastal Monitoring System (C-CEMS; Bonamano et al., 2016), whereas model outputs and satellite observations were provided by the CMEMS catalogue for the Mediterranean Sea products.

#### 2.2.1. In situ data

Between 2012 and 2017, in situ hydrographic surveys were performed in the study area. These surveys are part of the observation network, C-CEMS (Bonamano et al., 2016), which collects long-term observations and integrates data from fixed stations, satellite data and high-resolution coastal models. The C-CEMS network uses a specific set of platforms and numerical models (Marcelli et al., 2009) designed to capture the typical temporal and spatial scales of the Civitavecchia coastal areas, as proposed in Dickey and Bidigare (2005).

The in situ surveys were carried out from a small boat (5-m rigid inflatable) at a weekly frequency. During the experiments, the temperature, conductivity and fluorescence of chlorophyll *a* were measured at the observation station (OS, hereafter in the manuscript, red dot in Fig. 1c), located at  $42.08271^\circ\text{N}$ ,  $11.77738^\circ\text{E}$  1 nm off the Civitavecchia coast at a depth of 40 m using an Idronaut 316 plus multiparameter probe and a SeaPoint fluorometer. Details of the sampling surveys are described in Martellucci et al. (2018). Seawater samples were also collected to analyse chlorophyll *a* surface concentration according to the spectrophotometric method (Lorenzen, 1967; Lazzara et al., 1990) using a Shimadzu spectrophotometer UV mini 1240 model. In situ data were aligned with a 10 cm step and subsequently smoothed by a kernel function (using MATLAB® software). Salinity was computed using EOS 80 equations. Chlorophyll *a* concentrations were calculated by calibrating the fluorescence signal with spectrophotometric chlorophyll *a* concentration analysis. Solar radiation, rain, air pressure, wind speed (also used to calculate the wind stress) and wind direction were recorded by the C-CEMS weather station (see details in Zappalà et al., 2016).

#### 2.2.2. Model output data

Model output data for the investigated area were retrieved from the CMEMS catalogue using the analysis and reanalysis products for Mediterranean Sea physics and biogeochemistry delivered to CMEMS by the Mediterranean Sea Monitoring and Forecasting Centre (Med-MFC, see Clementi et al., 2017; Salon et al., 2019; Ravdas et al., 2018 for further details). We downloaded the CMEMS time series of daily temperature, salinity and chlorophyll *a* vertical profiles and waves at the model grid point closest to the OS of C-CEMS (blue dot in Fig. 1c). Two datasets were used: the multiyear reanalysis product at 1/16 degree (covering 1999–2016 at monthly frequency) and the near real time (NRT) analysis product at 1/24 degree (covering 2016–2018 at daily frequency). Model data, which have an uneven vertical spatial resolution, were interpolated to the vertical grid of observations and then used to complete the spatial autocorrelation analysis (Section 2.4). Interpolation, data spatial analysis and visualization were performed using Golden Software Surfer®.

#### 2.2.3. Satellite observations data

Satellite observation data for the study area were also retrieved from the CMEMS catalogue using the specific L3 and L4 ocean colour products

at a 1 km resolution for chlorophyll concentration (Volpe et al., 2019) and attenuation coefficient at 490 nm (Lee et al., 2002).

2.3. Empirical orthogonal function analysis of model and in situ vertical time series

The comparison between CMEMS model products and in situ C-CEMS observations was performed through the results of empirical orthogonal function (EOF) decomposition (Bjornsson and Venegas, 1997). The EOF decomposition provides a compact description of the temporal variability in the time series of vertical profiles, identifying a set of few orthogonal functions (vertical modes and their temporal evolution) that describe the largest fraction of the total variance.

We computed the EOF on the time series of the vertical profiles of temperature, salinity and chlorophyll *a* for both the model and in situ datasets. Specifically, the EOF analysis was performed using the MATLAB® function `caleof.m` (<https://www.mathworks.com>), which was applied to each data matrix after normalization, and log transformation for chlorophyll only. Normalization includes subtraction of the vertical mean and division by the standard deviation. Then, a comparison of the model and in situ data was accomplished by verifying the consistency (i. e., similarity) between the most informative statistical modes. Thus, the EOF analysis has allowed us to verify the consistency between the most relevant model and in situ data dynamics, despite the presence of biases and different spatiotemporal representative spectra between datasets.

2.4. Spatial autocorrelation analysis

The spatial extent of the representativeness of the OS in the surrounding area, also referred to as the “footprint” of a local observation system (Jones et al., 2015), was assessed by spatial multivariate

autocorrelation analysis. The correlation of each grid point of the coastal Tyrrhenian area with the OS was calculated for both model datasets: the monthly reanalysis, which provides a long-term scale, and the daily NRT model time series, which provides the short-term scale. The multivariate correlation  $\text{corr}(\text{MOD}_{X_{OS},Y_{OS}}, \text{MOD}_{X,Y})$  was computed considering the composite chlorophyll and nutrient (nitrate and phosphate) time series ( $\text{MOD} = [\text{CHL}(t), \text{NO}_3(t), \text{PO}_4(t)]$ ) at the OS point ( $X_{OS}, Y_{OS}$ ) and in any other point of the model domain; each variable is block normalized by the overall mean and standard deviation of each variable.

3. Results

3.1. Physical and biological characterization of the study area

Sea temperature vertical profile (Fig. 2) time series show definite seasonal variations characterized by cold and vertically mixed water columns, from mid-autumn to late spring, and thermally stratified water columns during the summer months. Both the duration and the intensity of mixing and stratification vary among different years. The lowest temperature occurs during the 2015 and 2017 winter seasons (14 °C), while during the 2016 winter, the water column presents a temperature higher than that in the other years (approximately 15 °C); this winter is also characterized by a mixing period longer than that in the other years. Summer warming generates stratification that allows the formation of a stable thermocline between 20 and 25 m depth. The 2015 summer presents the longest warm period, while the 2017 summer shows the highest temperature (26 °C). During summer, it is also possible to observe cooling of the subsurface layers, lifting the thermocline up towards the surface. This observation is more evident during August 2016, in which strong cooling involves the whole water column, reducing the temperature from 25 °C to 20 °C (see details in Martellucci

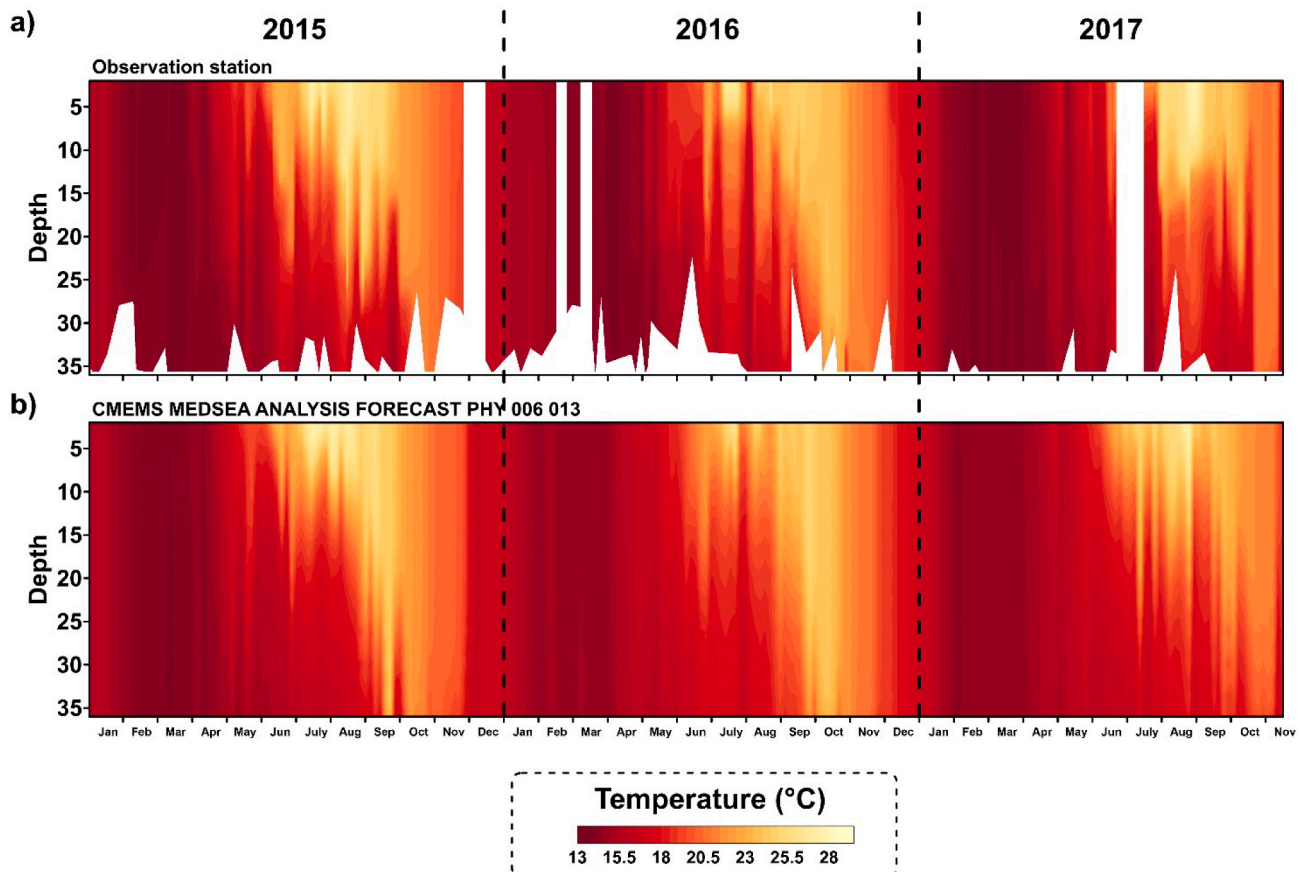


Fig. 2. Hovmöller diagram (y-depth/x-time) of temperature for OS (a) and model grid point (b).

et al., 2018). The autumn period is characterized by cooling of the water column: generally, at the end of November, the water column is well mixed and characterized by a temperature of approximately 21 °C.

The model (Fig. 2b) and in situ temperature observations (Fig. 2a) show a very good correlation ( $R^2 = 0.95$ ) in reproducing the temporal dynamics of temperature along the water column. The largest differences occur during summer and early autumn.

Salinity (Fig. 3) presents a high degree of variability, both in space (along the water column) and time (during the years). Salinity minima ( $36 \pm 0.2$  psu) are generally recorded in winter, where freshwater advection (Fig. 7a) causes a rapid and intense decrease in salinity concentrations, especially during 2015, resulting in a sharp halocline. Salinity maxima ( $38.2 \pm 0.2$  psu) occur during summer, and the increase mainly characterizes the surface layer. During the autumn season, terrestrial runoff produces a rapid salinity decrease in the surface layer, reaching approximately 37 psu, while salinity remains constant in the deep layer. During the analysed period, we may observe a general increase in the salinity concentration along the water column.

The model (Fig. 3b) and in situ observations (Fig. 3a) are in good agreement ( $R^2 = 0.76$ ): higher differences between the model and in situ observations are observed in the surface layer, especially during the winter period, while in the deep layer, the differences between the model and data are less than 0.2 psu.

The phytoplankton bloom episodes highlight spring and autumn blooms and show great differences between one year and another, presenting a great degree of variability in plankton biomass (Fig. 4). During early winter, phytoplankton are generally homogeneously distributed along the water column, presenting a chlorophyll *a* concentration of less than 0.5 µg/l. The onset of the spring bloom occurs at the beginning of February, which is when phytoplankton biomass achieved chlorophyll *a* concentrations larger than 2 µg/l; the highest

concentrations are observed in subsurface layers between 5 and 20 m depths.

During March, chlorophyll shows the highest variability: it is homogeneously distributed along the water column, and subsequently, chlorophyll *a* increases between 10 and 20 m depth, reaching the highest concentration at the beginning of April (2.5 µg/l). Generally, the spring bloom ends at the end of April. In late spring, it is possible to observe some limited (≈5 days) and subsurface (between 10 m and 20 m depth) blooms (e.g., May 2015 ≈ 1 µg/l and June 2016 ≈ 2 µg/l).

In detail, the 2015 spring bloom period is characterized by two blooms (5–25 m depth) that last approximately twenty days and present a horizontal extension of approximately 25 km (see also Fig. 8 for the integration with satellite images). The first bloom occurs in mid-February (≈2.5 µg/l), and the second bloom occurs at the end of March (≈2 µg/l), alternating with a period of chlorophyll minima along the water column (≈0.5 µg/l). The 2016 spring bloom does not present discontinuity; it involves the surface layers until 20 m depth and has a horizontal extension of approximately 15 km (Fig. 8). The bloom begins at the end of February and ends in early April; in this period, the chlorophyll *a* concentration is approximately 1.5 µg/l.

Four blooms occurred during the 2017 spring period, the chlorophyll patches involved almost the whole water column (5–30 m depth), and every single bloom presented a temporal extension of approximately 10/15 days. In particular, the first bloom occurred at the end of January (≈1 µg/l), the second was in mid-February (≈1.3 µg/l), the third was between February and March (≈3 µg/l) and the last bloom was at the end of March (≈2.5 µg/l). The first bloom was confined near the coast, while the last bloom presented a horizontal extension of approximately 10 km (Fig. 8).

During summer and until the beginning of the October surface layer, chlorophyll *a* disappears (i.e., the concentration is less than 0.1 µg/l),

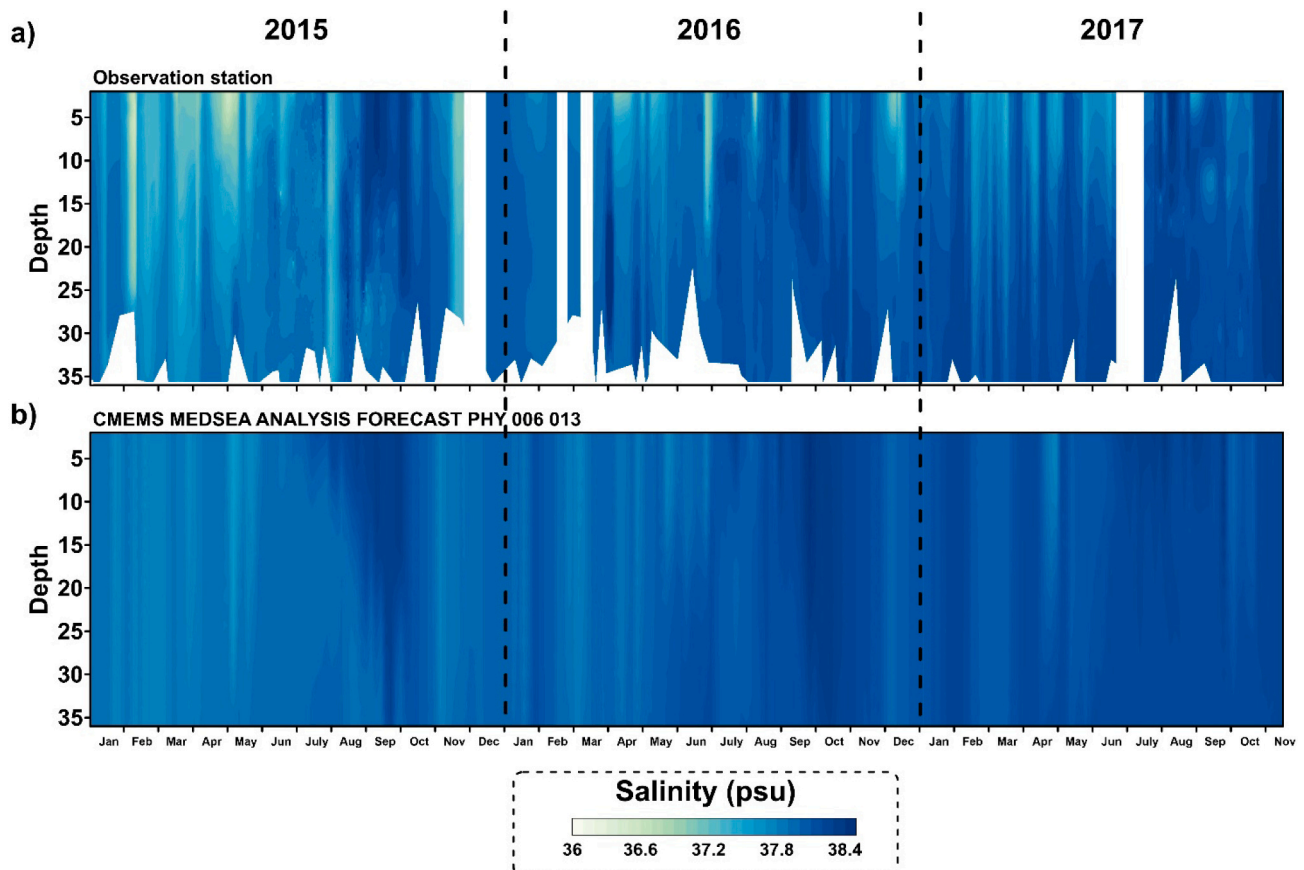


Fig. 3. Hovmöller diagram (y-depth/x-time) of salinity for OS (a) and model grid point (b).

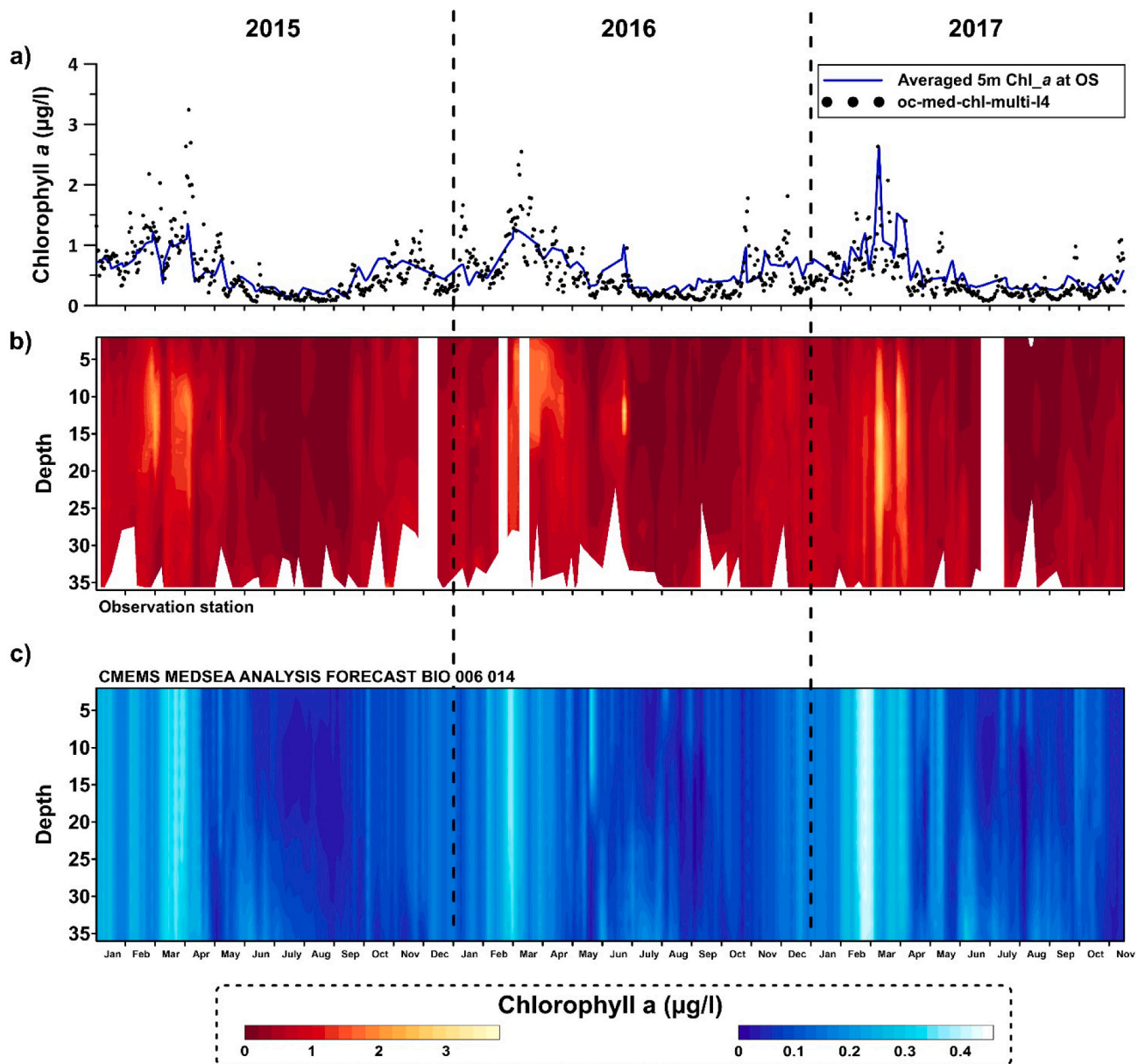


Fig. 4. Chlorophyll *a* time series measured at OS and Satellite (a) and Hovmöller diagram (y-depth/x-time) of chlorophyll *a* for OS (b) and model grid point (c).

while below the thermocline, a considerable concentration of chlorophyll *a* ( $<1 \mu\text{g/l}$ ) can be observed.

Autumn is characterized by a general increase in chlorophyll *a* concentration. These blooms are patchy and confined to the bottom layer below 20 m depth, presenting lower values than the spring bloom, with a maximum chlorophyll *a* concentration of approximately  $1.5 \mu\text{g/l}$  at deeper depths.

Satellite data (Fig. 4a) and model outputs (Fig. 4c) show the same trend as in situ observations (Fig. 4b), reproducing the temporal dynamics of chlorophyll. Compared with remote sensing, the highest differences occur during spring bloom episodes when satellite data overestimate in situ chlorophyll *a* concentrations. The model output shows good coherence with the observed temporal evolution, correctly reproducing the bloom episodes (see also Section 3.2, Fig. 5). However, a quantitative comparison spots a systematic underestimation of the modelled chlorophyll with winter and summer RMSD values equal to  $0.65$  and  $0.59 \text{ mgCHL/m}^3$ , respectively, and an error proportional to the biomass itself.

### 3.2. EOF analysis

The results of the EOF decompositions are shown in Fig. 5 and Table 1 for the C-CEMS in situ and CMEMS model time series. Generally, the first two modes explain up to 95% of the variance in the time series for all in situ and model variables (Table 1).

The first mode of temperature (an almost uniform negative profile) describes the temporal evolution of the seasonal cycle of heating and cooling of the water column. Both the model and in situ observations depict the temporal evolution of the first mode with maxima in winter and minima in summer. The first mode of the two datasets has a small discrepancy, showing the same trend both in situ and in model.

The second mode of temperature describes the onset of summer stratification and the abrupt change due to autumn vertical mixing: the temporal evolutions of the two datasets are well synchronized, and we can observe a continuous decrease during spring and summer and a sharp change in the sign of the temporal evolution in October (Fig. 5b and c).

The first salinity mode captures a barotropic term of decrease in

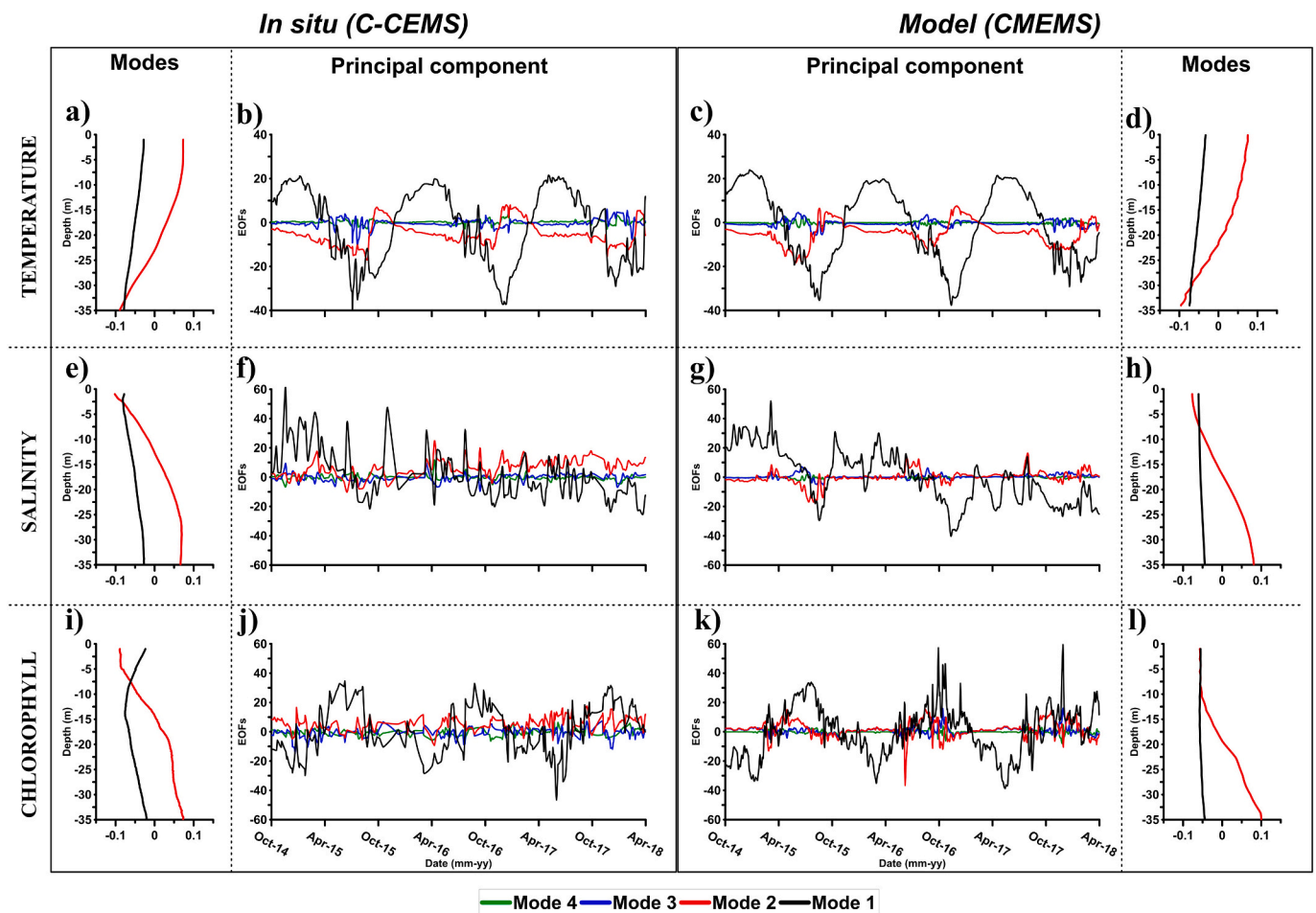


Fig. 5. First two spatial (a, d, e, h, i, l) and first four temporal (b, c, f, g, j, k) modes of the EOF decomposition for temperature, salinity and chlorophyll for in situ (left panels) and model data (right panel).

Table 1

Percent of explained variance of the first four modes of the EOF decomposition for model and in situ dataset variables.

Variable	In situ				Model			
	Mode 1	Mode 2	Mode 3	Mode 4	Mode 1	Mode 2	Mode 3	Mode 4
Temperature	82.8	15.9	1	0.2	84.9	14.1	0.7	0.1
Salinity	76.3	21.2	1.6	0.8	93.4	5.7	0.7	0
Chlorophyll	81.9	11.1	4.5	2.2	94.3	4.7	0.7	0.1

salinity due to external input related to river runoff, which is observable in both datasets, while the second mode describes a general vertical positive gradient along the whole water column. Model and in situ datasets are well synchronized: the temporal evolution of the salinity first mode shows the presence of several rain events and a negative tendency from 2015 to 2017, which is a common feature between the two datasets that is clearly visible in the Hovmöller diagrams in Fig. 3.

The EOF of the log-transformed model and in situ chlorophyll presented very high consistency. The first two modes (first mode up to 82% and 94% of the total variance, respectively, in situ and model) explain the occurrence of winter and autumn blooms, which impact the whole water column. On the other hand, the two second modes describe the general higher concentration at the bottom with respect to the surface during summer and autumn.

Despite some discrepancies (i.e., sharp oscillations in the in situ EOF whereas the model EOF is more regular, Fig. 5j and k), the seasonal cycle is well and consistently depicted by the temporal evolution of the first mode of the two datasets.

### 3.3. Spatial footprint of the OS

The footprint or representativeness of the OS is assessed by a multivariate autocorrelation analysis carried out on temperature, salinity and chlorophyll *a*. The results in Fig. 6 show that considering the long-term evolution extracted by the CMEMS reanalysis, the OS has a high correlation ( $R^2 > 0.85$ ,  $p < 0.0025$ ), with all the model grid points belonging to a large strip along the Tyrrhenian coast. The strip is up to 70–80 km in length, and the correlation identifies a typical seasonal cycle along the Tyrrhenian coast. However, a decrease in the correlation of the OS with the nearshore areas 30–40 km from the OS (i.e., north of Argentario and south of Santa Severa) can be noted.

Considering the time series of the NRT products at a higher resolution, the area showing a correlation higher than 0.85 with the OS point is much smaller. Its shape is elongated and northward oriented (i.e., it is as large as 20 km cross shore and 40–50 km along shore). Interestingly, the dynamics of the southern nearshore area are almost not correlated with the OS, showing that the plume of the Tiber River (i.e., the most

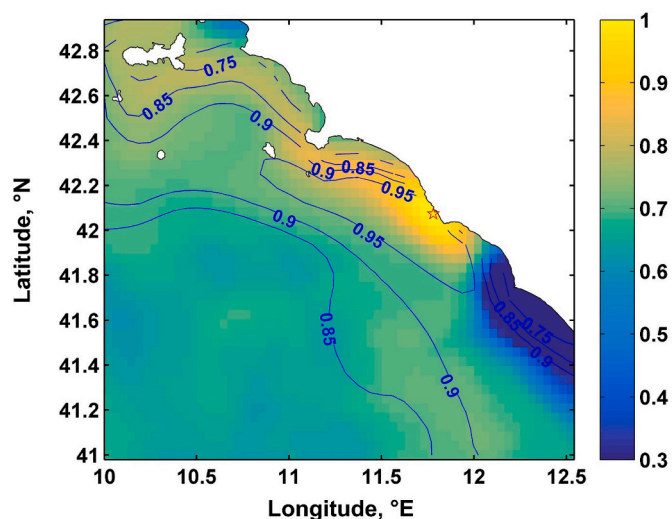


Fig. 6. Map of multivariate autocorrelation between the OS (red star) and each gridpoint of the model domain at surface. Correlation is computed from CMEMS reanalysis (blue contours and label) and Analysis and Forecast (coloured shaded area) datasets. (For interpretation of the references to colour in this figure legend, the reader is referred to the web version of this article.)

important river in the area, Fig. 1b) does not impact the dynamics of the OS.

### 3.4. External forcing (atmospheric and oceanic drivers)

The list of potential drivers for the bloom dynamics in the study area include the seasonal cycle of solar radiation, input of nutrients from rivers (here proxied by rain time series, as in Cossarini et al., 2008), optical depth, cross- and alongshore currents, mixed layer depth, wind stress (i.e., magnitude and direction) and significant wave height, which can be assumed to be an index of vertical mixing. The evolution of the drivers in the area is shown in Fig. 7, where the bloom events are depicted by green vertical bands.

Anticipated and concomitant forcings are quite different during the three investigated years, highlighting the importance of interannual variability in shaping the spatial-temporal scales of coastal bloom dynamics.

Solar radiation (Fig. 7a) shows the typical seasonal cycle of the temperate climate, and no significant variation is observed between one year and another. The optical depth time series (Fig. 7b) presents the same trend observed in solar radiation. In general, the highest variability occurs during the winter/spring season. Compared with the other summer periods, 2015 highlights the highest optical depth. Interestingly, the biomass increase occurred on June 2016, when we observed a reduction in the optical depth.

Rainy periods (Fig. 7a) occur during winter/spring and autumn seasons; however, significant interannual variability can be observed: 2017 reports much lower cumulative winter rain than 2015: 2821 mm/period in 2015, 1493 mm/period in 2016, and 795 mm/period in 2017.

The interannual cycle of wind stress highlights an elevated variability: 2017 reports the highest wind intensity, while 2016 shows a high intensity over a long period. The observed variability is reflected in the significant wave height time series (Fig. 7c): higher waves occur during winter concurrently with the highest wind stress, suggesting the presence of storms. This result strongly influences the mixed layer depth (MLD, Fig. 7b) that extends from the surface down to the bottom in winter and presents elevated variability.

## 4. Discussion

### 4.1. Impact of external forcing on phytoplankton annual cycles

In marine process studies, the knowledge of a phenomenon depends on observations, which are usually extremely complex because of the intrinsic difficulty of the type of measurements that have to be made (Crise et al., 2018). These issues are specifically urgent and strategic for coastal areas that present extremely high spatial-temporal variability. In this work, we aim to overcome the difficulties of the approach based on a limited set of observational tools by applying a multiplatform monitoring system (MPMS), which is synthesized in Fig. 8 for the study case, where different platforms are integrated to provide multiple scales and dimensions of the phenomena. Specifically, the local conditions are provided by the in situ data, the coast-open sea gradient at the surface are provided by satellite data and the vertical dynamics along the coast-open sea direction are provided by model outputs.

The phytoplankton dynamics observed in the study area seem to be similar, in both concentration and time, to those generally observed in the North Atlantic (Winder and Cloern, 2010; Cloern and Jassby, 2010) and in the Mediterranean Sea (Ribera et al., 2004; Zingone et al. 2010; Zingone et al., 2019), with regular seasonal patterns (i.e., spring and autumn blooms) and large interannual variability. The MPMS approach allows us to investigate the variability among the different years along both the horizontal and vertical planes, reflecting the variability in the drivers (e.g., hydrographic parameters), as typically expected for a coastal area to explain the Civitavecchia study case.

Fig. 8 shows the powerful approach of the integration proposed here: the three spring blooms highlight a great difference in the spatial and temporal extensions and in magnitude (as shown in Section 3.1), as clearly recognized in both the in situ observations and model output.

The environmental conditions (shown in Fig. 7) trigger blooms and can explain the variability observed in different years. During the 2017 spring bloom, the physical forcing presented the highest variability and magnitude, representing the most energetic conditions (i.e., daily wind stress and waves were the strongest). This result produces the highest variability observed in the 2017 blooms. On the other hand, the 2016 bloom presents the lowest variability, being driven by a weaker physical forcing (i.e., daily wind stress and waves): this bloom is triggered by an intense atmospheric event that occurred at the end of January 2016 and mixed the water column, producing the ideal environmental conditions for the onset of the bloom.

With respect to the other years, the 2015 spring bloom represents an intermediate condition in terms of physical forcing (i.e., variability and magnitude) and bloom characteristics. Following the physical forcing, the first bloom ends when an upwelling wind-driven event (6–9 March 2015; Martellucci et al., 2020) spreads the bloom offshore, and on successive days, the relaxation produces a second bloom (Fig. 8a).

The MPMS approach helps to understand the mechanisms that modulate locally observed phytoplankton dynamics. As observed in the literature, phytoplankton dynamics are triggered by external drivers such as wind, fronts, horizontal advection, and buoyancy fluxes (Kjørboe and Nielsen, 1990; Franks, 1992; Cloern, 1996; Franks and Chen, 1996; Lennert-Cody and Franks, 2002), which are much more variable in coastal environments than in the open ocean (Legendre and Demers, 1984; Cloern, 1996; Walsh, 1991; Ducklow and McCallister, 2005). This finding is especially true for the study area investigated here (Figs. 2, 3, 7), which is a transition zone influenced by river inputs (Piazzola et al. 2015), land use (Paladini de Mendoza et al., 2016; Marcelli et al., 2018), and exchanges with the open ocean related to the high interannual variability in Tyrrhenian Sea dynamics (Hopkins, 1988; Bakun and Agostini, 2001; Vetrano et al., 2010).

Many interesting considerations can be obtained by observing the evolution of the phytoplankton biomass (Fig. 4) related to external forcings (Figs. 2, 3 and 7) and comparing it with the available literature. The beginning of the spring bloom generally occurs during mid-



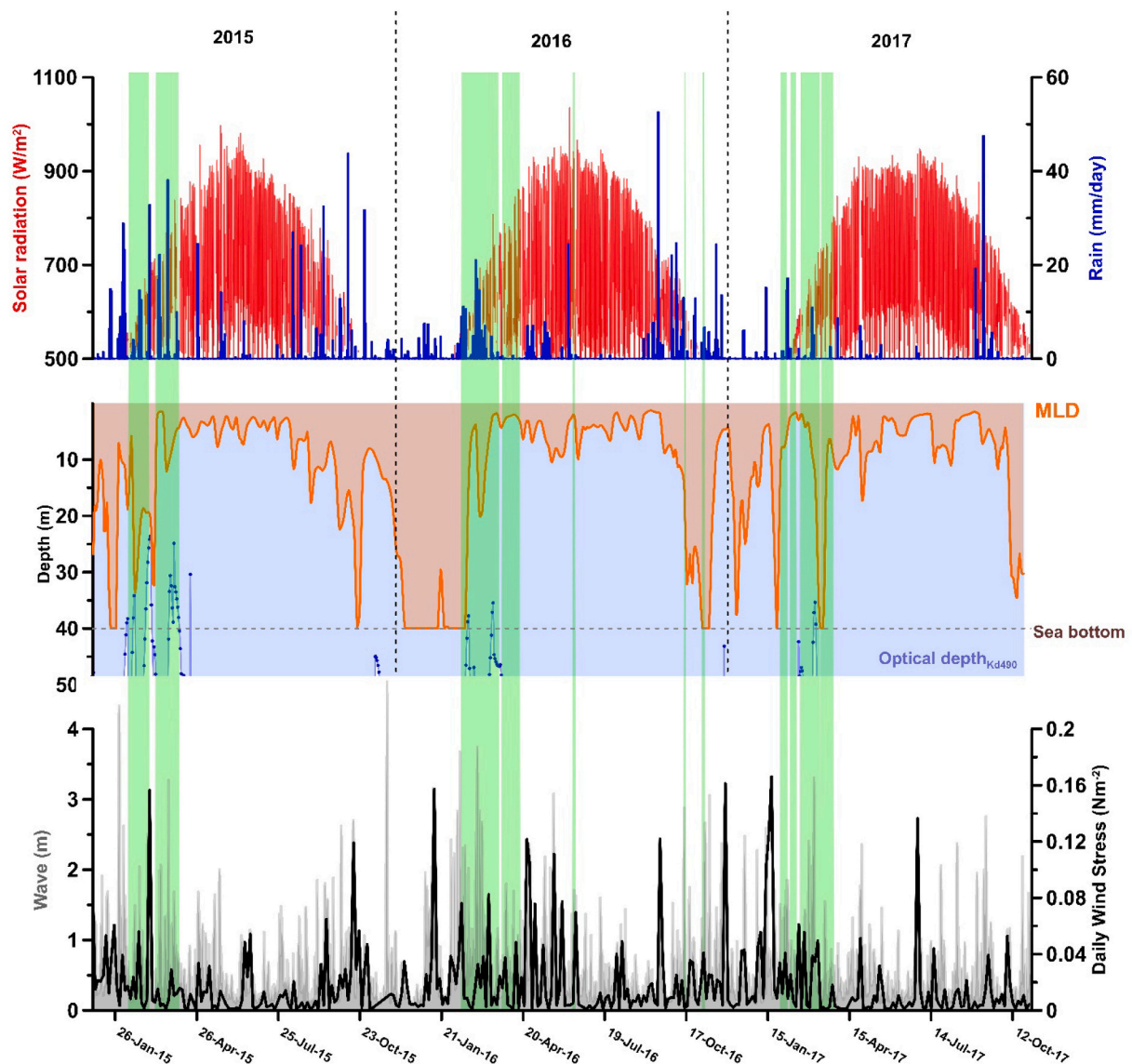


Fig. 7. Time series of external forcing, in the box on top (a) solar radiation (redline) daily rain (blue line); in the center box (b) optical depth (blue dotted line), mixed layer depth (orange filled line); in the box below (c) wind stress (black line) and significant wave height (grey line). The green rectangles that cross the boxes represent the spring bloom periods. (For interpretation of the references to colour in this figure legend, the reader is referred to the web version of this article.)

February, triggered by the increase in sunlight (overcoming a threshold of  $500 \text{ W/m}^2$ , Fig. 7a) and nutrients that are made available after winter mixing (Lévy et al., 1998) and quantified here by wind stress overcoming  $0.08 \text{ N/m}^2$  and significant wave heights higher than  $2 \text{ m}$  (Fig. 8c). During the early bloom, light input does not appear to be excessive (between  $500 \text{ W/m}^2$  and  $800 \text{ W/m}^2$ ) enough to cause photoinhibition phenomena, and the phytoplankton vertical structures involve the subsurface layer between  $10$  and  $25 \text{ m}$  depths. These patches are strongly influenced by both temperature (the  $14 \text{ }^\circ\text{C}$  isotherm limits chlorophyll abundance, as observed clearly during the 2015 and 2017 blooms when that isotherm encompasses the patches; Figs. 2 and 4) and salinity (higher concentrations occur with salinities ranging between  $37.5$  and  $38 \text{ psu}$ ; Figs. 3 and 4), which are mainly modulated by runoff dynamics (Fig. 7b). Indeed, the freshwater input produces both vertical mixing and higher turbidity (Simpson et al., 1991), limiting sunlight availability and reducing chlorophyll concentrations, as clearly observed in their decrease during 2015 and 2017 when salinity was lower than  $37.5 \text{ psu}$ , highlighting the freshwater impact in limiting chlorophyll patches. As typically observed in coastal systems (Franks, 1992; Franks and Chen, 1996; Franks and Walstad, 1997), the

chlorophyll maxima in Civitavecchia MPMS (Fig. 4) occur at the thermocline front (Fig. 2) both in their vertical displacement and duration.

Furthermore, we can speculate that the spring blooms may be related to the presence of diatoms, as observed in previous studies conducted in northern Tyrrhenian areas by Lenzi and Lazzara (1978), which are typically observed in cases of low temperature ( $<15 \text{ }^\circ\text{C}$ , Fig. 2), moderate salinity (between  $37.8$  and  $38$ , Fig. 3), low light (between  $500 \text{ W/m}^2$  and  $800 \text{ W/m}^2$ , Fig. 7b), and totally mixed water columns (Fig. 7b). The spring bloom ends when the sunlight exceeds  $800 \text{ W/m}^2$  and the water column structure changes from mixed to stratified (i.e., the decrease in MLD occurring in mid-April), which strengthens the hypothesis that they are diatoms. When the water column becomes more stratified, chlorophyll is generally distributed in the deep layer below the thermocline, in which the temperature is lower than  $16 \text{ }^\circ\text{C}$ . In the surface layer, chlorophyll presents concentrations near zero; indeed, in this period, the solar radiation is too high ( $>800 \text{ W/m}^2$ ) to allow for the growth of diatoms (Fig. 8).

The integrated analysis shows an increase in the subsurface layer chlorophyll concentrations during the early summer (2015 and 2016); these summer blooms were also previously observed in other studies

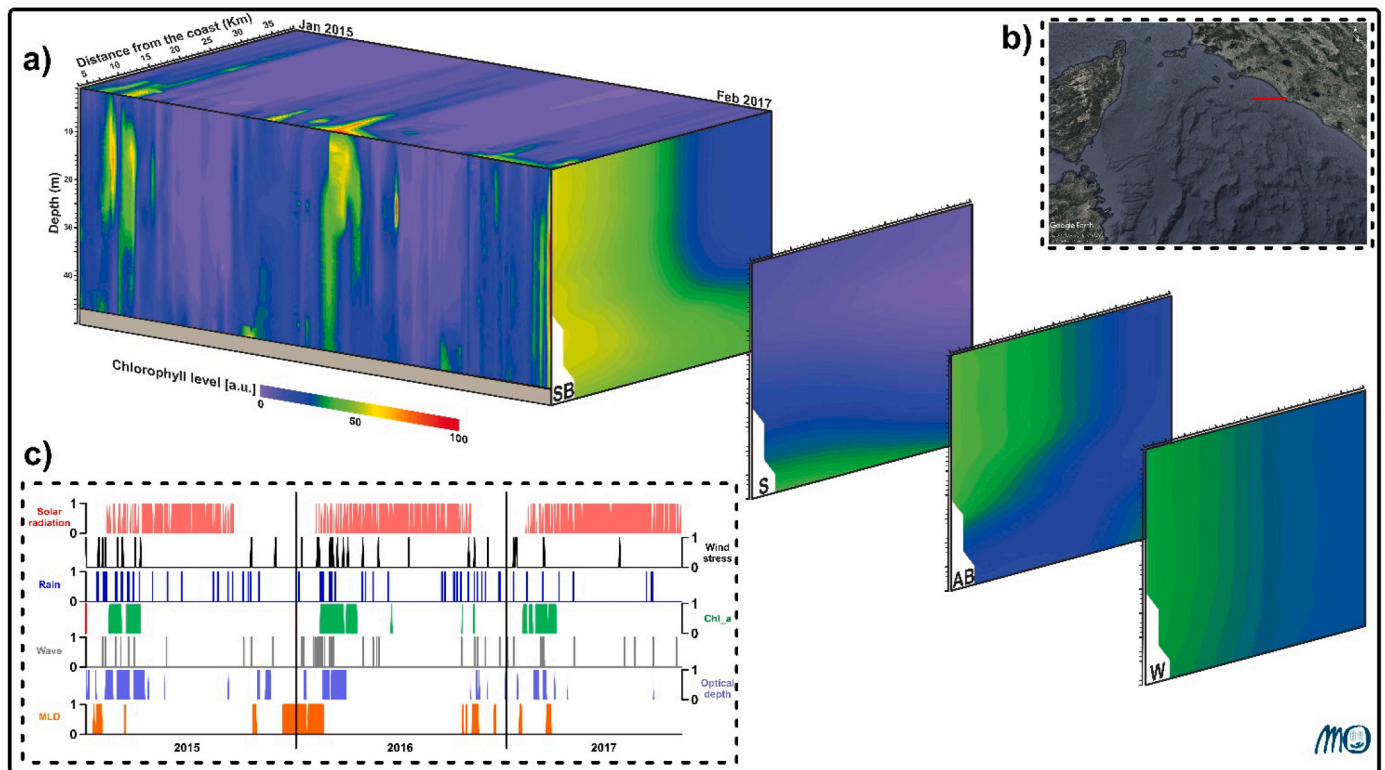


**Fig. 8.** Integration of different data sets: (a) Chlorophyll vertical and cross-shore representativeness of the MPMS. Backward face is chlorophyll from in situ data (y-depth/x-time); upward face is chlorophyll from satellite data (z-distance from coast/x-time) and sections are the average seasonal period from model outputs (y-depth/z-distance from coast), in which SB is the Spring Bloom period, S is Summer, AB is the Autumn Bloom and W is Winter. The colour scale is normalized between 0 and 100 for each dataset. (b) Location of the study area (the red line represents the section transect for satellite products). (c) Synthesis of external forcing time series based on blooming time (Fig. 7). They are represented as logical values (1 = true, 0 = false) based on the chosen threshold. The bloom period is defined with chlorophyll a concentrations greater than  $1 \mu\text{g l}^{-1}$ . Forcing thresholds are  $>500 \text{ W m}^{-2}$  for solar radiation,  $<60 \text{ m}$  for optical depth,  $>50 \text{ mm d}^{-1}$  for rain,  $>0.08 \text{ Nm}^{-2} \approx (7 \text{ ms}^{-1})$  for wind stress,  $>3 \text{ m}$  for waves, and  $>35 \text{ m}$  for MLD. (For interpretation of the references to colour in this figure legend, the reader is referred to the web version of this article.)

(Bernhard et al., 1969; Solazzi and Andreoli, 1971; Magazzù et al., 1975). Considering the high light level and the low turbulence (i.e., high stratification, low wind stress and waves), typical of the summer season (Martellucci et al., 2018), these blooms could be due to the presence of dinoflagellates, which are typical of the warm season, as previously observed in the northern Tyrrhenian area by Lenzi and Lazzara (1978, 1980). Moreover, these blooms seem to end when intense freshwater discharge causes a decrease in salinity concentrations, increasing turbulence and as an ecological consequence, limiting dinoflagellate growth.

The autumn period is characterized by stormy events that generate precipitation and waves (Trigo et al., 2006; Ulbrich et al., 2012; Paladini de Mendoza et al., 2018), producing intense mixing that breaks the summer stratification (i.e., the isothermal displacement during the autumn period, clearly observed in both observations and model outputs; Fig. 2). This mixing can increase nutrient availability, producing a second annual bloom (typical of mid latitudes; Zingone et al., 1995). In the OS, the chlorophyll patch is confined below the 20 m depth, and the environmental conditions (i.e., low temperature, high salinity and mixing) suggest the presence of diatoms, which, similarly to spring, dominate the autumn period, as observed by Lenzi and Lazzara (1978, 1980). However, the low level of chlorophyll observed during autumn blooms suggests that nutrient availability is not enough to produce the high chlorophyll levels observed in spring.

#### 4.2. Integration of multiplatform datasets

Our approach, which includes in situ, satellite and model data, is

targeted to consider all the available information necessary to sustainably operate efficient coastal ecosystem monitoring. This includes local in situ infrastructure costs (Cristini et al., 2016; Marcelli et al., 2009), which have to be planned to maintain the monitoring operations, and benefits from the publicly available data paradigm based on the CMEMS service, which provides the regional-scale products (model outputs and satellite data). The proposed best practice framework is quantitative and supported by the proven consistency among different datasets, which usually give different representations of the investigated site (i.e., as already seen in Section 3: the in situ station shows only the very local dynamics, the satellite observes only the surface layer during cloud-free periods, and the model tends to underestimate the in situ chlorophyll data).

The framework is based on the definition of the processes to be investigated and followed by a 4-step procedure, whose main elements are described in Table 2, and characterizes the methodology used, as well as the specific application for the Civitavecchia coastal MPMS, aimed to investigate the dynamics of phytoplankton blooms here.

Preliminarily (step 0 in Table 2), the investigated phenomena must be defined in terms of the major variables involved and the spatial and temporal dimensions (Levin, 1992; Dickey and Bidigare, 2005). Then, the first step is site characterization based on the literature and historical data and background site analysis (e.g., Fig. 1). The MPMS data collection (step 2) aims to gather all available data useful for the analysis. In our case, from the analysis of the in situ OS long-term data, we can characterize the investigated site by its seasonal dynamics, typical atmospheric and oceanic drivers, and interannual variability: the datasets we gathered cover the local observation network area, which has a

**Table 2**

Proposed best practice layout for multi-platform approach. Each item is mapped onto the specific element for the application to the investigated site.

Element of best practice	Relevant methodology	Proposed application to case study of Civitavecchia coastal MPMS for period 2015–2017
0. Definition of the process to be investigated	Variables. Temporal dimension (frequency and length of the time series monitoring). Spatial dimension (synoptic levels).	Interannual variability of phytoplankton blooms in the Tyrrhenian coastal area
1. Characterization of the study site	Background analysis based on literature and other available historical data.	Morphodynamic properties. Oceanographic and atmospheric characteristics. Socio-economic aspects.
2. MPMS data collection	Long-term in situ qualified multi-variable time series data provided by a coastal OS (e.g. monitoring surveys, gliders, moorings...). Data for the characterization of the mean state and the seasonal variability of the investigated site, with definition of the typical atmospheric and oceanic drivers. Satellite data. Model data.	Time series of daily means of the vertical profile of Temperature, Salinity and Chlorophyll (based on C-MEMS data) seasonal variability of wind, air temperature, precipitation, river inputs, ocean current, MLD (based on C-CEMS and literature data). Daily means of Chlorophyll content in the surface layer (based on CMEMS OC products). Daily means of 3-D fields of Temperature, Salinity, Chlorophyll (based on CMEMS MED products).
3. Consistency analysis among multi-platform datasets	Use of EOF and multi-variate correlation analysis.	Robustness quantitatively built on EOF results for Temperature, Salinity and Chlorophyll, multivariate autocorrelation analysis between OS and model data (Figs. 5 and 6).
4. Integrated and coherent multi-variate analysis to extract information on the investigated process	Statistical analysis of external drivers, spatial interpolation, temporal evolution analysis.	Multi-variate phenomenological analysis of phytoplankton blooms process (Figs. 7 and 8).

spatial scale of O (1 km). Satellite data and modelling results allow us to enlarge our analysis to a wider area, including the mesoscale (O (10 km), which is of the order of the Rossby Radius in the central Tyrrhenian Sea; [Vetrano et al., 2010](#)). Furthermore, satellite and model data can highlight possible large-scale relationships to explain the observed interannual variability in phytoplankton blooms.

The consistency among the MPMS datasets (step 3) is provided by the EOF analysis, which quantifies the coherence among the different data streams, showing that the three multiplatform data streams (in situ, satellite and model) describe, with their own limits, the same seasonal dynamics, thus justifying the MPMS approach. Additionally, by highlighting possible inconsistencies among the datasets, our multiplatform integrated approach provides a useful method for investigating specific sensors or model failures. Indeed, our analysis highlighted that the CMEMS model, while correctly reproducing phytoplankton dynamics, systematically underestimates the high level of chlorophyll that can be observed at nearshore observation sites. The inspection of [Fig. 4](#) (i.e., error proportional to the phytoplankton biomass) points towards the model parameterization controlling the optical characteristics and the carbon to chlorophyll dynamics. As the CMEMS model is tailored for basin-wide Mediterranean oligotrophic conditions ([Lazzari et al., 2012](#); [Salon et al., 2019](#)), achieving an appropriate level of validation at

multiple spatial scales (i.e., from coastal to open sea and at different horizontal resolutions) with a complex biogeochemical model featuring a global uniform parameterization is not a straightforward task.

Multivariate autocorrelation analysis may provide significant indications of the representativeness of OS. Establishing the link between the local submesoscale observations, based on the C-CEMS observational network, and the mesoscale drivers, provided by CMEMS products, is part of the integration of the MPMS (step 4). Visual representation of multivariate temporal evolution (e.g., [Fig. 7](#)), spatial multidimensional integration (e.g., [Fig. 8](#)) and statistical analysis allow us to analyse the temporal and spatial scales of variability in the processes under investigation. Our aim to investigate the interannual variability in phytoplankton blooms in the Tyrrhenian coastal area is thus realized by the spatial 3-dimensional extent of the coastal blooms ([Fig. 8](#)) and the occurrence and intensity of the drivers (multivariate temporal analysis shown in [Fig. 7](#)).

However, future developments of the CMEMS marine operational system aimed to serve quantitatively the coastal monitoring, would highly benefit from the specific skill assessment that our approach provides.

## 5. Conclusions

The analysis of the time series of phytoplankton provided by in situ, satellite and model data for the Civitavecchia MPMS shows the typical dynamics of the coastal temperate systems, which are characterized by spring and autumn blooms and significant interannual variability. Following our data integration approach, the EOF analysis has extensively shown consistency among the multiplatform datasets. Notwithstanding the incongruences related to model representativeness error (i.e., river nutrient inputs based on climatological information and coarse grid resolution), the intercomparison is beneficial to provide information on phytoplankton dynamics and drivers at different temporal and spatial scales. Indeed, in situ data describe the very local dynamics by integrating all the on-site physical and biogeochemical processes, satellite data provide the evolution of the large-scale surface chlorophyll patterns at high resolution, and the model extends the 3-D structure of the physical and biogeochemical processes, quantifying the role of the different drivers.

Through the study of the dynamics of coastal blooms in the Civitavecchia coastal system (Tyrrhenian Sea), we present one of the first examples that allows us to assess the CMEMS model accuracy at the local and coastal scaled, enriching the basin-wide skill performance assessment of the Mediterranean Sea system. Finally, we propose a best practice framework that can potentially be applied to any MPMS to provide a better understanding of coastal phenomena deeper than that provided by any individual dataset.

## Declaration of Competing Interest

None.

## Acknowledgements

This study has been conducted using EU Copernicus Marine Service Information. The authors thank to the Civitavecchia Port Authority for funding the implementation of C-CEMS, and in particular to Calogero Burgio, Giorgio Fersini and Maurizio Marini. We would like to thank Dr. Alberto Pierattini for data acquisition, Dr. Cristiano Melchiorri for data analysis and the scientific illustrator Dr. Matteo Oliverio for graphical abstract and [Fig. 8](#).

## References

- Allen, J.I., Holt, J.T., Blackford, J., Proctor, R., 2007. Error quantification of a high-resolution coupled hydrodynamic-ecosystem coastal-ocean model part 2.

- Chlorophyll-a, nutrients and SPM. *J. Mar. Syst.* 68, 381–404. <https://doi.org/10.1016/j.jmarsys.2007.01.005>.
- Anselmi, B., Benvegna, F., Brondi, A., Ferretti, O., 1978. Classificazione geomorfologica delle coste italiane come base per l'impostazione di studi sulla contaminazione marina. In: Atti III Congresso A.I.O.L., Sorrento, Italy, 18–20 December 1978.
- Astraldi, M., Gasparini, G.P., 1994. The seasonal characteristics of the circulation in the Tyrrhenian Sea. In: La Violette, P.E. (Ed.), *Seasonal and Interannual Variability of the Western Mediterranean Sea*. American Geophysical Union, Washington DC, pp. 115–134. <https://doi.org/10.1029/CE046p0115>.
- Astraldi, M., Bianchi, C.N., Gasparini, G.P., Morri, C., 1995. Climatic fluctuations, current variability and marine species distribution a case study in the Ligurian Sea (north-west Mediterranean). *Oceanol. Acta* 18, 139–149.
- Bakun, A., Agostini, V.N., 2001. Seasonal patterns of wind-induced upwelling/downwelling in the Mediterranean Sea. *Sci. Mar.* 65 (3), 243–257. <https://doi.org/10.3989/scimar.2001.65n3243>.
- Bernhard, M., Rampi, L., Zattera, A., 1969. La distribuzione del Fitoplancton nel Mar Ligure. *Pubblicazioni Stazione Zoologica Napoli* 37, 73–114.
- Bjornsson, H., Venegas, S.A., 1997. A manual for EOF and SVD analyses of climate data. In: CCGCR Report No. 97-1, Montréal, Québec. McGill University, 52 pp.
- Bonamano, S., Piermattei, V., Madonia, A., Paladini de Mendoza, F., Pierattini, A., Martellucci, R., Stefanì, C., Zappalà, G., Marcelli, M., 2015. The Civitavecchia Coastal Environment Monitoring System (C-CEMS) a new tool to analyse the conflicts between coastal pressures and sensitivity areas. *Ocean Sci.* 12, 87–100. <https://doi.org/10.5194/os-12-87-2016>.
- Bonamano, S., Madonia, A., Borsellino, C., Stefanì, C., Caruso, G., De Pasquale, F., Piermattei, V., Zappalà, G., Marcelli, M., 2016. Modeling the dispersion of viable and total *Escherichia coli* cells in the artificial semi-enclosed bathing area of Santa Marinella (Latium, Italy). *Mar. Pollut. Bull.* 95 (1), 141–154. <https://doi.org/10.1016/j.marpolbul.2015.04.030>, 15.
- Brondi, A., Ferretti, O., Anselmi, B., Falchi, G., 1979. Analisi granulometriche e mineralogiche dei sedimenti fluviali e costieri del territorio italiano. *Boll. Soc. Geo. It.* 98, 293–326.
- Chiocci, F.L., La Monica, G.B., 1996. Analisi sismostratigrafica della piattaforma continentale. In: Il Mare del Lazio. Università degli Studi di Roma “La Sapienza”, Regione Lazio Assessorato Opere e Reti di Servizi e Mobilità, Tip. Borgia (Ed), Roma, pp. 40–61.
- Clementi, E., Oddo, P., Drudi, M., Pinardi, N., Korres, G., Grandi, A., 2017. Coupling hydrodynamic and wave models first step and sensitivity experiments in the Mediterranean Sea. *Ocean Dyn.* 67, 1293–1312. <https://doi.org/10.1007/s10236-017-1087-7>.
- Cloern, J.E., 1996. Phytoplankton bloom dynamics in coastal ecosystems a review with some general lessons from sustained investigation of San Francisco bay, California. *Rev. Geophys.* 34, 127–168. <https://doi.org/10.1029/96RG00986>.
- Cloern, J.E., Jassby, A.D., 2010. Patterns and scales of phytoplankton variability in estuarine-coastal ecosystems. *Estuar. Coasts* 33230–33241. <https://doi.org/10.1007/s12237-009-9195-3>.
- Cossarini, G., Libralato, S., Salon, S., Gao, X., Giorgi, F., Solidoro, C., 2008. Downscaling experiment for the Venice lagoon. II. Effects of changes in precipitation on biogeochemical properties. *Clim. Res.* 45, 43–59. <https://doi.org/10.3354/cr00758>.
- Crise, A., Ribera d'Alcalá, M., Mariani, P., Petihakis, Robidart, J., Iudicone, D., Bachmayer, R., Malfatti, F., 2018. A conceptual framework for developing the next generation of marine Observatories (MOBs) for science and society. *Front. Mar. Sci.* <https://doi.org/10.3389/fmars.2018.00318>.
- Cristini, L., Lampitt, R.S., Cardin, V., Delory, E., Haugan, P., O'Neill, N., Petihakis, G., Ruhl, H.A., 2016. Cost and value of multidisciplinary fixed-point ocean observatories. *Mar. Policy* 71, 138–146. <https://doi.org/10.1016/j.marpol.2016.05.029>.
- De Angelis, C.M., 1956. Ciclo del Fitoplancton del Golfo di Napoli. *Boll. Pesca Piscic. Idrobiol.* 2, 5–20.
- Dickey, T.D., Bidigare, R.R., 2005. Interdisciplinary oceanographic observations: the wave of the future. *Sci. Mar.* 69 (Suppl. 1), 23–42.
- Ducklow, H.W., McCallister, L., 2005. The biogeochemistry of carbon dioxide in the coastal oceans. In: Robinson, A.R., McCaerthy, P.J., Rothschild, B.J. (Eds.), *The Sea*, 13. John Wiley & Sons, New York, pp. 269–305. ISBN 0-471-18901-4.
- Elliot, A.J., 1981. Low frequency current variability off the West coast of Italy. *Oceanol. Acta* 4 (1), 47–55.
- Franks, P.J.S., 1992. Phytoplankton blooms at fronts patterns, scales, and physical forcing mechanisms. *Rev. Aquat. Sci.* 6 (2), 121–137.
- Franks, P.J.S., Chen, C., 1996. Plankton production in tidal fronts a model of Georges Bank in summer. *J. Mar. Res.* 54, 631–651.
- Franks, P.J.S., Walstad, L.J., 1997. Plankton patches at fronts a model of formation and response to wind events. *J. Mar. Res.* 55, 1–29. <https://doi.org/10.1357/0022240973224472>.
- Gattuso, J.P., Frankignoulle, M., Wollast, R., 1998. Carbon and carbonate metabolism in coastal aquatic ecosystems. *Annu. Rev. Ecol. Syst.* 29, 405–434. <https://doi.org/10.1146/annurev.ecolsys.29.1.405>.
- Hardman-Mountford, N., Allen, J.I., Frost, M.T., Hawkins, S.J., Kendall, M.A., Mieszkowska, N., Richardson, K., Somerfield, P.J., 2005. Diagnostic monitoring of a changing environment an alternative UK perspective. *Mar. Pollut. Bull.* 50, 1463–1471. <https://doi.org/10.1016/j.marpolbul.2005.06.022>.
- Hays, G.C., Richardson, A.J., Robinson, C., 2005. Climate change and marine plankton. *TRENDS Ecol. Evol.* 20 (6 June 2005).
- Hopkins, T.S., 1988. Recent observation on the intermediate and deep water circulation in the southern Tyrrhenian Sea. *Oceanol. Acta* 9, 41–50.
- Iacono, R., Napolitano, E., Marullo, S., Artale, V., Vetrano, A., 2013. Seasonal variability of the Tyrrhenian Sea surface geostrophic circulation as assessed by altimeter data. *J. Phys. Oceanogr.* 43, 1710–1732. <https://doi.org/10.1175/JPO-D-12-0112.1>.
- Innamorati, M., Lazzara, L., Nuccio, C., De Poi, M., Mannucci, M., Mori, G., 1990. Biomassa fitoplanctonica e condizioni idrologiche nell'Alto Tirreno Toscano. In: *Resoconti dei rilevamenti in mare*, n.7. Dipartimento di Biologia Vegetale, Firenze, pp. 1–95.
- Innamorati, M., Lazzara, L., Nuccio, C., Mori, G., Massi, L., Cherici, V., 1992. Il fitoplancton dell'alto Tirreno condizioni trofiche e produttive. In: Atti del 9° congresso A.I.O.L., S. Margherita Ligure, 20–23 Novembre 1990, pp. 199–205.
- Jones, E.M., Doblin, M.A., Matear, R., King, E., 2015. Assessing and evaluating the ocean-colour footprint of a regional observing system. *J. Mar. Syst.* 143, 49–61. <https://doi.org/10.1016/j.jmarsys.2014.10.012>.
- Kjørboe, T., Nielsen, T.G., 1990. Effects of wind stress on vertical water column structure, phytoplankton growth, and productivity of planktonic copepods, in Trophic relationships in the marine environment. In: *Proc 24th European Marine Biology Symposium*. Aberdeen University Press, pp. 28–40.
- La Monica, G.B., Raffi, R., 1996. Morfologia e sedimentologia della spiaggia e della piattaforma continentale interna. In: Il Mare del Lazio, Università degli Studi di Roma “La Sapienza”, Regione Lazio Assessorato Opere e Reti di Servizi e Mobilità, Tip. Borgia (Ed), Roma, pp. 62–105.
- Lazzara, L., Bianchi, F., Falucci, M., Hull, V., Modigh, M., Ribera d'Alcalá, M., 1990. Pigmenti clorofilliani. *Nova Thalassia*, 11, pp. 207–223.
- Lazzari, P., Solidoro, C., Ibbello, V., Salon, S., Teruzzi, A., Béranger, K., Colella, S., Crise, A., 2012. Seasonal and interannual variability of plankton chlorophyll and primary production in the Mediterranean Sea: a modelling approach. *Biogeosciences* 9, 217–233. <https://doi.org/10.5194/bg-9-217-2012>.
- Le Traon, P.Y., Reppucci, A., Alvarez, F., Fanjul, E., Aouf, L., Behrens, A., Belmonte, M., Benkiran, M., 2019. From observation to information and users: the Copernicus Marine Service perspective. *Front. Mar. Sci.* 6, 234.
- Lee, Z., Carder, K., Arnone, R., 2002. Deriving inherent optical properties from water color: a multiband quasi-analytical algorithm for optically deep waters. *Appl. Opt.* 41, 5755–5772. <https://doi.org/10.1364/AO.41.005755>.
- Legendre, L., Demers, S., 1984. Towards dynamic biological oceanography and limnology. *Can. J. Fish. Aquat. Sci.* 41, 2–19.
- Lennert-Cody, C.E., Franks, P.J.S., 2002. Fluorescence patches in high-frequency internal wave. *Mar. Ecol. Prog. Ser.* 235, 29–42. <https://doi.org/10.3354/meps235029>.
- Lenzi, Grillini C., Lazzara, L., 1978. Ciclo annuale del fitoplancton nelle acque costiere del Parco Naturale della Maremma I. Variazioni quantitative. *G. Bot. Ital.* 112 (3), 157–173.
- Lenzi, Grillini C., Lazzara, L., 1980. Ciclo annuale del fitoplancton nelle acque costiere del Parco Naturale della Maremma II. Flora e variazioni delle comunità. *G. Bot. Ital.* 114, 199–215.
- Levin, S.A., 1992. The problem of pattern and scale in ecology: the Robert H. MacArthur Award Lecture. *Ecology* 73 (6), 1943–1967. <https://doi.org/10.2307/1941447>.
- Lévy, M., Mémyer, L., André, J.M., 1998. Simulation of primary production and export fluxes in the northwestern Mediterranean Sea. *J. Mar. Res.* 56, 197–238.
- Liu, K.-K., Iseki, K., Chao, S.-Y., 2000. Continental margin carbon fluxes. In: Hanson, R. B., Ducklow, H., Field, J.G. (Eds.), *The Changing Ocean Carbon Cycle: A Midterm Synthesis of the Joint Global Ocean Flux Study*, International Geosphere-Biosphere Programme Book Series, 5. Cambridge Univ. Press, New York, pp. 187–239, 7.
- Lorenzen, C.J., 1967. Determination of chlorophyll and phaeo-pigments spectrophotometric equations. *Limnol. Oceanogr.* 12, 343–346.
- Magazzù, G., Andreolli, C., Munaò, F., 1975. Ciclo annuale del Fitoplancton e della produzione primaria del basso Tirreno. *Mem. Biol. Mar. Oceanogr.* 5, 25–48.
- Marcelli, M., Caburazzi, M., Perilli, A., Piermattei, V., Fresi, E., 2005. Deep chlorophyll maximum distribution in the central Tyrrhenian Sea described by a towed undulating vehicle. *Chem. Ecol.* 21, 351–367.
- Marcelli, M., Peviani, M., Piermattei, V., Carli, F., Bonamano, S., 2009. Sea-use map of Italy: Gis supporting marine energy siting. In: *Proceedings of the European Seminar “Offshore Wind and Other Marine Renewable Energies in Mediterranean and European Seas”*, Brindisi, Italy, 21–23 May 2009.
- Marcelli, M., Scanu, S., Manfredi, Frattarelli F., Maria, Mancini E., Carli, F., 2018. A benthic zonation system as a fundamental tool for natural capital assessment in a marine environment a case study in the northern Tyrrhenian Sea, Italy. *Sustainability* 10 (10), 3786. <https://doi.org/10.3390/su10103786>.
- Margalef, R., 1978. Life-form of phytoplankton as survival alternatives in an unstable environment. *Oceanol. Acta* 1, 493–509.
- Margalef, R., Estrada, M., Blasco, D., 1969. Functional morphology of organisms involved in red tides, as adapted to decaying turbulence. In: Taylor, D.L., Seliger, H. H. (Eds.), *Toxic Dinoflagellate Blooms*. Elsevier/North Holland, New York, pp. 89–94.
- Martellucci, R., Pierattini, A., Paladini de Mendoza, F., Melchiorri, C., Piermattei, V., Marcelli, M., 2018. Physical and biological water column observations during summer sea/land breeze winds in the coastal northern Tyrrhenian Sea. *Water* 10, 1673. <https://doi.org/10.3390/w10111673>.
- Martellucci, R., Menna, M., Piermattei, V., Marcelli, M., 2020. Evidences of coastal upwelling along the northeastern Tyrrhenian coast. (personal communication).
- Mozetić, P., Solidoro, C., Cossarini, G., Socal, G., Precali, R., Francé, J., Umani, S.F., 2010. Recent trends towards oligotrophication of the northern Adriatic: evidence from chlorophyll a time series. *Estuar. Coasts* 33 (2), 362–375.
- Muller-Karger, F.E., Varela, R., Thunell, R., Luerssen, R., Hu, C., Walsh, J.J., 2005. The importance of continental margins in the global carbon cycle. *Geophys. Res. Lett.* 32. Nuccio, C., Innamorati, M., Lazzara, L., Mancuso, A., 1995. Distribuzione spaziale e stagionale delle cenosi fitoplanctoniche nel Tirreno Settentrionale. In: Atti della

- Società Toscana di Scienze Naturali. Lo stato degli ecosistemi marini del Tirreno Toscano, Grosseto 2-4 Dicembre 1993, Grafiche Pacini editore.
- Oesterwind, D., Rau, A., Zaiko, A., 2016. Drivers and pressures – untangling the terms commonly used in marine science and policy. *J. Environ. Manag.* 181, 8–15. <https://doi.org/10.1016/j.jenvman.2016.05.058>.
- Oinonen, S.B., Hynes, T., Buchs, S., Heiskanen, A., Hyytiäinen, A.S., Luisetti, K., Veeren, T., 2016. The role of economics in ecosystem based management: the case of the EU marine strategy framework directive; first lessons learnt and way forward. *J. Ocean Coastal Econ.* 2 <https://doi.org/10.15351/2373-8456.1038>.
- Paladini de Mendoza, F., Bonamano, S., Stella, G., Giovacchini, M., Capizzi, D., Fraticelli, F., Muratore, S., Burgio, C., Scanu, S., Peviani, M.A., Marcelli, M., 2016. Where is the best site for wave energy exploitation? Case study along the coast of northern Latium (ITALY). *J. Coast. Conserv.* <https://doi.org/10.1007/s11852-015-0414-8>, 2013–29.
- Paladini de Mendoza, F., Fontolan, G., Mancini, E., Scanu, E., Scanu, S., Bonamano, S., Marcelli, M., 2018. Sediment dynamics and resuspension processes in a shallow-water *Posidonia oceanica* meadow. *Mar. Geol.* 404, 174–186. <https://doi.org/10.1016/j.margeo.2018.07.006>.
- Piazzolla, D., Scanu, S., Frattarelli, F.M., Mancini, E., Tiralongo, F., Brundo, M.V., Tibullo, D., Pecoraro, R., Copat, C., Ferrante, M., Marcelli, M., 2015. Trace-metal enrichment and pollution in coastal sediments in the northern Tyrrhenian Sea, Italy. *Arch. Environ. Contam. Toxicol.* 69 (4), 3–14. <https://doi.org/10.1007/s00244-015-0166-3>.
- Piazzolla, D., Cafaro, V., Mancini, E., Scanu, S., Bonamano, S., Marcelli, M., 2020. Preliminary investigation of microlitter pollution in low-energy hydrodynamic basins using *Sabella spallanzanii* (Polychaeta: Sabellidae) tubes. *Bull. Environ. Contam. Toxicol.* 104, 345–350. <https://doi.org/10.1007/s00128-020-02797-x>.
- Pinardi, N., Navarra, A., 1993. Baroclinic wind adjustment processes in the Mediterranean Sea. *Deep-Sea Res. II* 40 (6), 1299–1326.
- Poulain, P.M., Menna, M., Mauri, E., 2012. Surface Geostrophic circulation of the Mediterranean Sea derived from drifter and satellite altimeter data. *J. Phys. Oceanogr.* 42 (6), 973–990. <https://doi.org/10.1175/JPO-D-11-0159.1>.
- Ravdas, M., Zacharioudaki, A., Korres, G., 2018. Implementation and validation of a new operational wave forecasting system of the Mediterranean Monitoring and Forecasting Centre in the framework of the Copernicus Marine Environment Monitoring Service. *Nat. Hazards Earth Syst. Sci.* 18, 2675–2695. <https://doi.org/10.5194/nhess-18-2675-2018>.
- Ribera, D'alcalá M., Conversano, F., Corato, F., Licandro, P., Mangoni, O., Marino, D., Mazzocchi, M.G., Modigh, M., Montresor, M., Nardella, M., Saggiomo, V., Sarno, D., Zingone, A., 2004. Seasonal patterns in plankton communities in a pluriannual time series at a coastal Mediterranean site (Gulf of Naples) an attempt to discern recurrences and trends. *Sci. Mar.* 68, 65–83. <https://doi.org/10.3989/scimar.2004.68s165>.
- Salon, S., Cossarini, G., Bolzon, G., Feudale, L., Lazzari, P., Teruzzi, A., Solidoro, C., Crise, A., 2019. Novel metrics based on Biogeochemical Argo data to improve the model uncertainty evaluation of the CMEEMS Mediterranean marine ecosystem forecasts. *Ocean Sci.* 15 (997–1022), 2019. <https://doi.org/10.5194/os-15-997-2019>.
- Scanu, S., Paladini de Mendoza, F., Piazzolla, D., Marcelli, M., 2015. Anthropogenic impact on river basins temporal evolution of sediment classes and accumulation rates in the northern Tyrrhenian Sea, Italy. *Oceanol. Hydrobiol. St.* 44 (1), 74–86. <https://doi.org/10.1515/ohs-2015-0008>.
- Seibert, S.L., Degenhardt, J., Ahrens, J., Reckhardt, A., Schwalfenberg, K., Waska, H., 2020. Investigating the land-sea transition zone. In: Jungblut, S., Liebich, V., Bode-Dalby, M. (Eds.), *YOUMARES 9 - The Oceans: Our Research, Our Future*. Springer, Cham.
- Simpson, J.H., Sharples, J., Rippeth, T.P., 1991. A prospective model of stratification induced by freshwater runoff. *Estuar. Coast. Shelf Sci.* 33, 23–35.
- Solazzi, A., Andreolli, C., 1971. Produttività e ciclo annuale del Fitoplancton del Medio Adriatico Occidentale. In: *Quad. Ab. Tecn. Pesca C.N.R. Ancona*, 1, pp. 1–90.
- Trigo, R., Xoplaki, E., Zorita, E., Luterbacher, J., Krichak, S.O., Alpert, P., Jacobeit, J., Sáenz, J., Fernández, J., González-Rouco, F., García-Herrera, R., Rodó, X., Brunetti, M., Nanni, T., Maugeri, M., Türke, M., Gimeno, L., Ribera, P., Brunet, M., Trigo, I.F., Crepon, M., Mariotti, A., 2006. Relations between variability in the Mediterranean region and mid-latitude variability. In: Lionello, P., Malanotte-Rizzoli, P., Boscolo, R. (Eds.), *Mediterranean Climate Variability*. Elsevier, Amsterdam, pp. 179–226. [https://doi.org/10.1016/S1571-9197\(06\)80006-6](https://doi.org/10.1016/S1571-9197(06)80006-6).
- Ulbrich, U., Lionello, P., Belusic, D., Jacobeit, J., Knippertz, P., Kuglitsch, F.G., Leckebusch, G.C., Luterbacher, J., Maugeri, M., Maheras, P., Nissen, K., Pavan, V., Pinto, P., Saaroni, H., Seubert, S., Toreti, A., Xoplaki, E., Ziv, B., 2012. Climate of the Mediterranean synoptic patterns, temperature, precipitation, winds, and their extremes. In: Lionello, P. (Ed.), *The Climate of the Mediterranean Region. From the Past to the Future*. Elsevier, London, pp. 301–346.
- de la Vara, A., del Sastre, P.G., Arsouze, T., Gallardo, C., Gaertner, M.Á., 2019. Role of atmospheric resolution in the long-term seasonal variability of the Tyrrhenian Sea circulation from a set of ocean hindcast simulations (1997–2008). *Ocean Model* 134, 51–67. <https://doi.org/10.1016/j.ocemod.2019.01.004>.
- Vetrano, A., Napolitano, E., Iacono, R., Schroeder, K., Gasparini, G.P., 2010. Tyrrhenian Sea Circulation and water mass fluxes in spring 2004 observations and model results. *J. Geophys. Res.* 115, C06023. <https://doi.org/10.1029/2009JC005680>.
- Volpe, G., Colella, S., Brando, V.E., Forneris, V., La Padula, F., Di Cicco, A., Santoleri, R., 2019. Mediterranean ocean colour level 3 operational multi-sensor processing. *Ocean Sci.* 15 (1), 127–146.
- Walsh, J.J., 1988. *On the Nature of Continental Shelves*. Academic Press.
- Walsh, J.J., 1991. Importance of continental margins in the marine biogeochemical cycling of carbon and nitrogen. *Nature* 350, 53–55.
- Winder, M., Cloern, J., 2010. The annual cycles of phytoplankton biomass. *Philos. Trans. R. Soc. Lond. Ser. B Biol. Sci.* 365, 3215–3226. <https://doi.org/10.1098/rstb.2010.0125>.
- Zappalà, G., Piermattei, V., Madonia, A., Martellucci, R., Bonamano, S., Pierattini, A., Burgio, C., Marcelli, M., 2014. Assessment of environmental conditions in Civitavecchia (Rome) harbour. In: Brebbia, C.A. (Ed.), *Water Pollution XII, Transaction Ecology And The Environment*, 182. <https://doi.org/10.2495/WP140241.4>.
- Zappalà, G., Caruso, G., Bonamano, S., Madonia, A., Piermattei, V., Martellucci, R., Di Cicco, A., Pannocchi, A., Stefani, C., Borsellino, C., Marcelli, M., 2016. A multi-platform approach to marine environment assessment in Civitavecchia (Rome) area. *J. Oper. Oceanogr.* 9 (sup1), 131–143. <https://doi.org/10.1080/1755876X.2015.1119561>.
- Zingone, A., Casotti, R., Ribera, D'alcalá M., Scardi, M., Marino, D., 1995. "St Martin's summer" the case of autumn phytoplankton bloom in the gulf of Naples (Mediterranean Sea). *J. Plankton Res.* 17, 575–593.
- Zingone, A., Phipps, E.J., Harrison, P.J., 2010. Multiscale variability of twenty-two coastal phytoplankton time series a global scale comparison. *Estuar. Coasts* 33, 224–229. <https://doi.org/10.1007/s12237-009-9261-x>.
- Zingone, A., D'Alelio, D., Mazzocchi, M.G., Montresor, M., Sarno, D., LTER-MC Team, 2019. Time series and beyond multifaceted plankton research at a marine Mediterranean LTER site. In: Mazzocchi, M.G., Capotondi, L., Freppaz, M., Lugliè, A., Campanaro, A. (Eds.), *Italian Long-Term Ecological Research for Understanding Ecosystem Diversity and Functioning. Case Studies From Aquatic, Terrestrial and Transitional Domains*. Nature Conservation, 34, pp. 273–310. <https://doi.org/10.3897/natureconservation.34.30789>.